Chemical Science

ROYAL SOCIETY OF CHEMISTRY

EDGE ARTICLE

View Article Online
View Journal | View Issue

Check for updates

Cite this: *Chem. Sci.*, 2025, **16**, 21950

All publication charges for this article have been paid for by the Royal Society of Chemistry

Design principles of spacer cations for suppressing phase segregation in 2D halide perovskites

Seonhong Min,[a] Manish Mukherjee,[bc] Gábor Szabó,[bc] Prashant V. Kamat *[bcd] and Junsang Cho *[a]

Suppression of photoinduced halide segregation in mixed halide perovskites remains a significant challenge for their application as wide bandgap semiconductors in solar cells. In addition to stability issues, halide segregation leads to a loss in power conversion efficiency in solar cells and a shift in emission wavelength in light-emitting devices. However, employing low-dimensional halide perovskites, such as two-dimensional (2D) or quasi-2D structures, offers a strategy to mitigate this segregation. Here, we have systematically studied how the molecular structure and binding configuration of spacer cations, ranging from linear alkyl chains to aromatic structures, affect photoinduced halide segregation across both Ruddlesden–Popper (RP) and Dion–Jacobson (DJ) frameworks in 2D mixed halide perovskites (Br : I = 50 : 50). Aromatic spacer cations within the DJ perovskite configuration were found to suppress segregation most effectively. For example, the halide segregation rate in a 2D mixed halide perovskite film with the DJ phase using the aromatic spacer cation 1,4-phenylenedimethanammonium (PDMA) was 9.3×10^{-4} s^{-1}—an order of magnitude lower than that observed with linear 2D RP perovskites employing butylammonium (BA) as the spacer cation (6.1×10^{-3} s^{-1}). Spectroscopic studies detailing the influence of spacer cation selection in mixed halide perovskites for suppressing phase segregation are discussed.

Received 25th August 2025
Accepted 10th October 2025

DOI: 10.1039/d5sc06511a

rsc.li/chemical-science

Open Access Article. Published on 21 1404. Downloaded on 28/11/1404 10:53:09 ..
This article is licensed under a Creative Commons Attribution-NonCommercial 3.0 Unported Licence.

Introduction

Two-dimensional (2D) lead halide perovskites, which emerge as counterparts to three-dimensional (3D) perovskites, have generated significant research interest in developing photovoltaics,[1,2] light-emitting diodes,[3,4] X-ray scintillators,[5] photodetectors,[6,7] and other applications.[8–12] Such lower-dimensional halide perovskites are composed of two different components, including intercalated organic spacer cations (S) and inorganic lead octahedral slabs $[PbX_6]^{4-}$. In general, 2D perovskites can be categorized into three groups including (1) Ruddlesden–popper, with a chemical formula of $S_2A_{n-1}B_nX_{3n+1}$; S = butylammonium (BA), benzylammonium (BzA), phenethylammonium (PEA), (2) Dion–Jacobson, $S'A_{n-1}B_nX_{3n+1}$; S′ = 1,4-butanediamminium (BDA), 1,4-phenylenedimethanammonium (PDMA), and (aminomethyl)piperidinium (AMP), and (3) alternating cation interface, $S''A_nB_nX_{3n+1}$; S″ = guanidium (GA), respectively, wherein B is a divalent metal (Pb^{2+} or Sn^{2+}); X is a halide (Cl^-, Br^-, I^-, or a mixture of them); and n is the inorganic layer number.[13–16] Importantly, the main distinction between RP and DJ perovskites lies in the crystallographic alignment of inorganic slabs. While the RP phases feature a staggered arrangement of adjacent slabs separated by van der Waals gaps, the DJ phases display directly connected inorganic slabs in an eclipsed manner.[17–19] Increased degree of freedom to modulate either organic or inorganic components makes such materials versatile, thus allowing the tailoring of the desired optoelectronic properties with enhanced stability. Specifically, the lead octahedral layer thickness number (n) is tunable, modulating the exciton binding energy, bandgap, and photoluminescence (PL) emission wavelength.[8,20–22] Depending on the type of intercalated organic spacer molecules and their valence state, the stability of 2D halide perovskites can be quite determined.[23–27]

Under continuous light irradiation, mixed halides (Br/I) undergo halide phase segregation with the formation of Br- and I-rich domains.[28–32] The halide phase segregation results in charge carrier cascade and funneling into the lower bandgap I-rich phase, thus decreasing the power conversion efficiency of solar cells and causing red-shifted emission in light-emitting diodes.[33,34] Thus, halide ion migration and halide phase segregation remain challenges to overcome in devices, since they directly influence the device stability under operational conditions.[11,35,36] While the introduction of 2D perovskites on top of

[a]*School of Energy and Chemistry, Sungshin Women's University, Seoul 01133, South Korea. E-mail: jcho3@sungshin.ac.kr*

[b]*Notre Dame Radiation Laboratory, University of Notre Dame, Notre Dame, Indiana 46556, USA. E-mail: pkamat@nd.edu*

[c]*Department of Chemistry and Biochemistry, University of Notre Dame, Notre Dame, Indiana 46556, USA*

[d]*Department of Chemical and Biomolecular Engineering, University of Notre Dame, Notre Dame, Indiana 46556, USA*

© 2025 The Author(s). Published by the Royal Society of Chemistry

Open Access Article. Published on 21 1404. Downloaded on 28/11/1404 10:53:09 ..
This article is licensed under a Creative Commons Attribution-NonCommercial 3.0 Unported Licence.

3D structures or the formation of quasi-2D perovskites effectively suppresses ion migration, due to intrinsic halide ion mobility arising from soft ionic lattices, halide ion segregation can still occur within a 3D framework under continuous light illumination.[37–40] The photoinduced iodine migration could ultimately lead to iodine expulsion from the perovskite lattices. For example, halide perovskite films in contact with solvents such as dichloromethane or dichloroethane and under bandgap excitation, exhibit expulsion of iodine into the solution as I_3^- species.[24,41–43]

Significant research efforts have been devoted to suppressing halide segregation in 3D perovskites (ABX_3; $A^+ = Cs^+$, methylammonium (MA^+), formamidinium (FA^+)) through A-site cation engineering,[44] B-site cation engineering,[45,46] X-site anion engineering,[31,47] and introduction of surface capping ligands with defect passivation.[48–51] The defect-mediated halide ion migration proceeds through sequential processes involving initial iodide (I^-) oxidation to neutral iodine ($I^\bullet$), trapping of iodine ($I^\bullet$) at interstitial sites, and corresponding iodide vacancy (I_V^+) formation.[52–57] In a similar fashion, 2D mixed halide perovskites also exhibit photoinduced halide segregation with intercalated spacer cations playing a crucial role in regulating phase segregation behavior.[23,42] In the case of RP perovskites, enhanced van der Waals interactions between spacer ligands, achieved through the introduction of π rings, extended chain lengths, and heteroatoms (*viz.* F or S) into the spacer molecular structures, have been found to be effective in rigidifying the 2D lattice frameworks.[58–60] In addition, the glass transition temperature of spacer ligands dictates the degree of halide ion migration since halide ion diffusion is initiated upon the disorder and melting of the spacer ligand assembly.[27,61–65]

Although the intercalated spacer cations in 2D perovskites do not directly alter the bandgap and optoelectronic properties, certain molecular descriptors of 2D spacer molecular design indeed influence the mixed halide stability. Specifically, variations in charge distribution, charge carrier lifetime, and dipolar polarization in spacer cation molecules influence the halide ion transport across the 2D perovskite lattice along the in-plane direction.[16,66–69] A fundamental question arises as to how these molecular structures and binding configurations determine the degree of halide ion migration within these 2D perovskites. We have now probed photoinduced halide ion segregation in the 2D mixed lead halide perovskites ($n = 1$). The halide ion mobility dependence on spacer cation molecules can provide fundamental insight into designing rules and proper selection of spacer cations with improved stability of perovskites. Our approach paves the way for the development of improved performance of perovskite optoelectronics along with long-term device stability.

Results and discussion

Molecular structures of spacer cations in 2D perovskites

The advantage of 2D halide perovskites is centered around the versatility of structural tunability. This specific property enables modulation of inorganic layers and various types of organic spacer cations. Although the spacer molecules are known not to impact the bandgap and optoelectronic properties directly, the molecular structures and binding configuration of spacers indeed govern the stability of 2D halide perovskites.[18] Fig. 1A and B exhibit the two representative 2D halide perovskites: Ruddlesden–Popper (RP) and Dion–Jacobson (DJ) phases, respectively, depending on the valence state of spacer cations. A monodentate (monovalent cation) spacer is employed in the RP structure to make a van der Waals gap of 2D structures, while the bidentate (divalent cation) spacer can enable more tight covalent binding onto 2D perovskites.

To systematically understand the impact of molecular structures and binding configuration on stabilizing the mixed halide perovskites, we employed well-known RP (butylamine (BA) and benzylamine (BzA)) and DJ spacers (1,4-butylenediamine (BDA) and 1,4-phenylenediamine (PDMA)), respectively. Fig. 1C shows the corresponding XRD patterns of these 2D layered perovskites, similar to 2D quantum well structures.[9] The periodic repetition of the interlayer spacing along (00l) crystallographic planes is observed with a periodicity of 6.3 (BA), 5.9 (BzA), 8.8 (BDA), and 7.3° (PDMA), respectively. Each interlayer distance spacing can be calculated using Bragg's equation ($n\lambda = 2d \sin\theta$) and was determined to be 1.4 (BA), 1.5 (BzA), 1.0 (BDA), and 1.2 nm (PDMA), respectively. The interlayer spacing distance is mainly determined by the size of intercalated spacer molecules—BA (0.6 nm), BzA (0.7 nm), BDA (0.75 nm), and PDMA (and 0.85 nm)—and the fixed length of a single layer of lead octahedral slabs: $[PbBr_6]^{4-}$ = 0.58 nm and $[PbI_6]^{4-}$ = 0.63 nm. Note that within the same binding configuration of spacers (RP or DJ), the linear ligands (BA and BDA) show a shorter interlayer spacing compared to bulkier aromatic ligands (BzA and PDMA).[26] Additionally, 2D DJ perovskites exhibit a much reduced interlayer spacing of 1.0–1.2 nm compared to 2D RP perovskites of 1.4–1.5 nm, since the bidentate nature of ligands eliminates the van der Waals gaps.

To further understand the influence of spacer cation on the binding energy of the [Pb–X] bond, X-ray photoelectron spectroscopy was performed. The XPS spectra shown in Fig. 1D and E exhibit the evolution of Pb 4f and I 3d signals in these 2D perovskite films. XPS spectra for Br 3d are also provided in Fig. S1 (SI). Given the fixed halide composition (Br : I = 50 : 50), the Pb–X binding energy is directly influenced by the molecular structure with corresponding electron density of spacer cations.[27] The binding energy of Pb $4f_{7/2}$ observed in 2D perovskite films was determined to be 137.8 (BA), 138.3 (BzA), 137.3 (BDA), and 137.8 eV (PDMA), respectively (Fig. 1D and Table S1).

In general, the aromatic spacer cations (compared to aliphatic ones), regardless of binding configuration, induce stronger binding of the Pb atom in the 2D perovskite lattices due to increased electron density on the Pb atom. The same trends were also seen in the binding energies of I $3d_{5/2}$ and Br $3d_{5/2}$ (Fig. 1E and S1). Interestingly, when the binding configuration shifted from RP (monodentate) to DJ (bidentate), both the binding energy of Pb 4f and other halide 3d levels decreased (Fig. 1D and E). A binding energy shift of −0.5 eV was seen in both cases when the binding configuration of spacer cations transitioned from RP to DJ (for linear BA *vs.* BDA) and −0.5 eV (for aromatic BzA *vs.* PDMA), respectively. Increased valence charge of spacer cations

Open Access Article. Published on 21 1404. Downloaded on 28/11/1404 10:53:09 ..
This article is licensed under a Creative Commons Attribution-NonCommercial 3.0 Unported Licence.

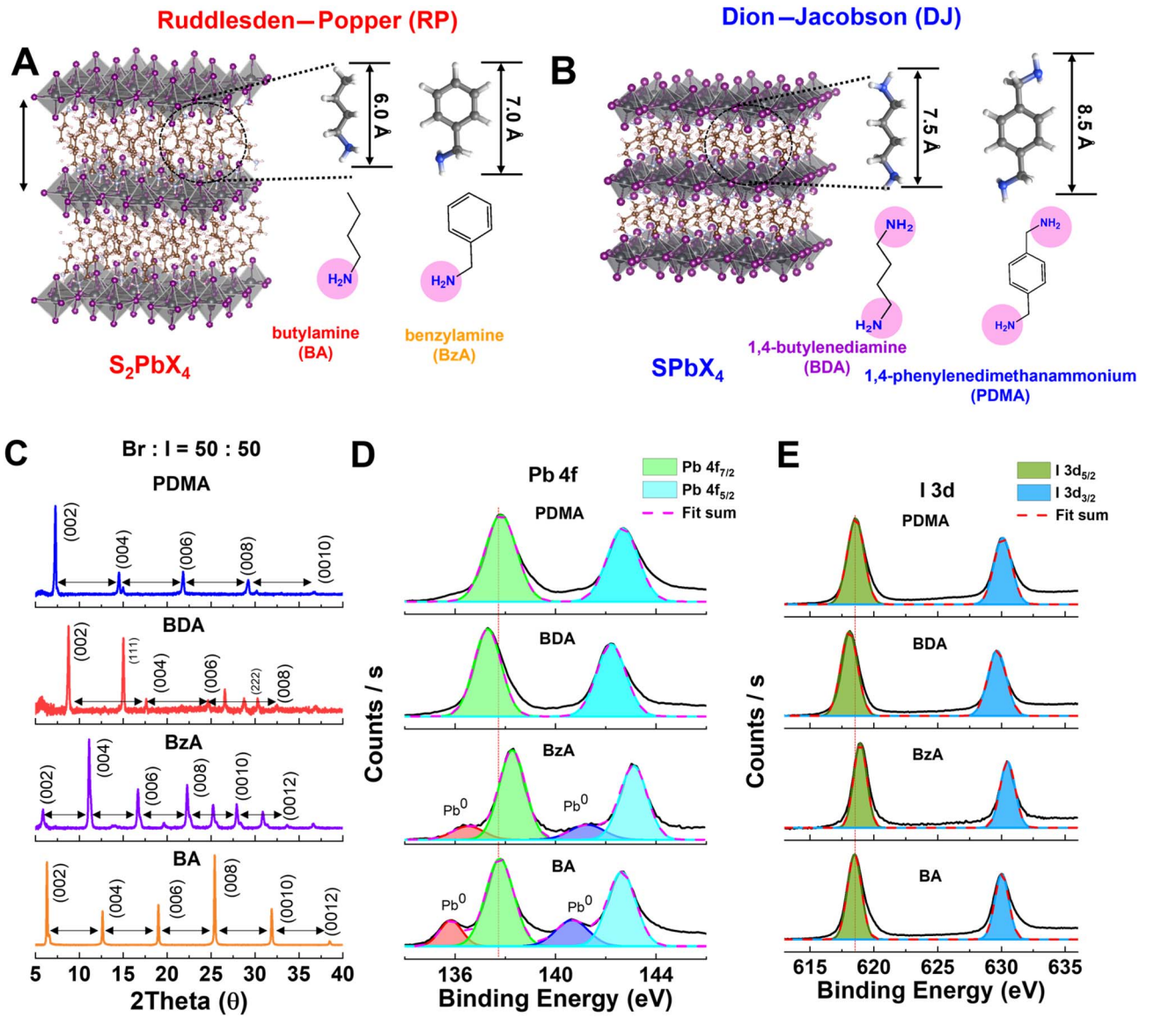

Fig. 1 (A and B) Crystal structures of 2D RP perovskites with a formula of S_2PbX_4 (A) and 2D DJ perovskites with a formula of $SPbX_4$ (B). (C) XRD patterns obtained for 2D mixed halide perovskites of Br : I = 50 : 50 with BA, BzA, BDA, and PDMA as spacers. (D and E) XPS spectra for Pb 4f and I 3d recorded for 2D mixed halide perovskites with BA, BzA, BDA, and PDMA as spacers from bottom to top.

from monovalent RP^+ to divalent DJ^{2+} spacer molecules can indeed withdraw the electron density from the Pb–X bond. These results reflect that the DJ spacer cations are more tightly bound toward the electron density over the Pb–X bonds. It is also worth mentioning that the DJ configuration significantly suppresses the formation of metallic Pb^0 that is often observed in RP perovskites due to undercoordinated Pb atom in the lattices (Fig. 1D). These observations were corroborated by SEM images, which show that introduction of tighter binding DJ spacers exhibit the reduced defect density along with a relatively increased grain size (Fig. S2).

Excited state properties

Optical properties of the 2D mixed halide perovskites were characterized using absorption and photoluminescence (PL) spectra (Fig. 2A–F). The absorption spectra of RP and DJ films of 2D perovskites are characterized by pronounced band-edge absorption around 445–450 nm across all samples (Fig. 2A and B). Insets in Fig. 2A and B show the digital photographs taken for these two films, indicative of similar bandgaps displaying yellow colors. The absorption spectra of 2D pure 100% Br and 100% I perovskites for comparison are presented in the SI (Fig. S3A–D). Based on the band-edge peak and bandgap shift as a function of halide composition, the 2D mixed Br : I = 50 : 50 films exhibit an intermediate bandgap between 100% Br and 100% I films (Fig. S3E). It is worth noting that 2D perovskites with aromatic spacer cations exhibit a slightly blue-shifted absorption peak compared to their counterparts with aliphatic ligands. The increased binding energy of Pb–X appears to induce stronger quantum confinement effects. Based on the bandgaps of 2D perovskites with pure bromide and iodide, the

© 2025 The Author(s). Published by the Royal Society of Chemistry

Open Access Article. Published on 21 1404. Downloaded on 28/11/1404 10:53:09 ..
This article is licensed under a Creative Commons Attribution-NonCommercial 3.0 Unported Licence.

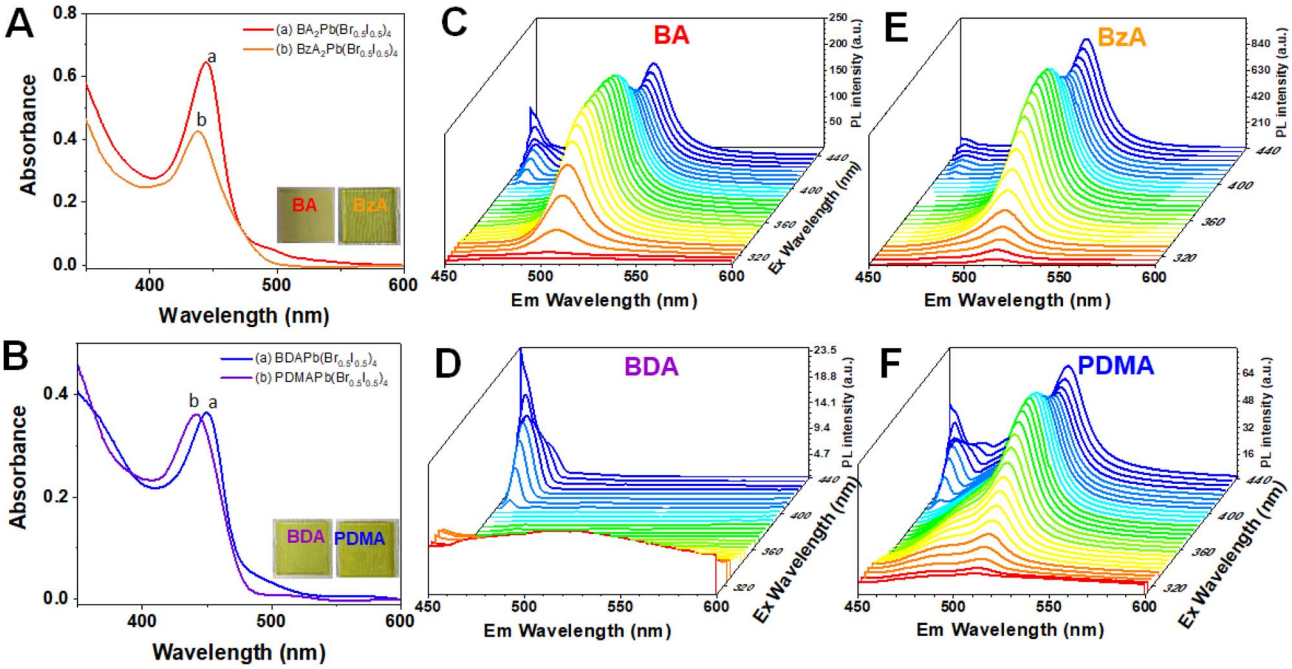

Fig. 2 (A and B) UV-vis absorption spectra of 2D mixed (Br : I = 50 : 50) halide perovskite films: (A) 2D RP perovskites with BA and BzA and (B) 2D DJ perovskites with BDA and PDMA. (C–F) 2D photoluminol excitation–emission spectra recorded for 2D perovskite films with varying spacer cations: (C) $BA_2Pb(Br_{0.5}I_{0.5})_4$, (D) $BDAPb(Br_{0.5}I_{0.5})_4$, (E) $BzA_2Pb(Br_{0.5}I_{0.5})_4$, and (F) $PDMAPb(Br_{0.5}I_{0.5})_4$, respectively. All films were excited over the 300–440 nm wavelength range, and emissionwas recorded between 450–600 nm.

bandgap predicted for Br : I = 50 : 50 composition using Vegard's law was closely matched with the experimentally measured values across all 2D perovskites (Fig. S3F).

These halide perovskites can be excited at the band edge or above the bandgap to characterize their emissive properties. 2D excitation–emission spectra recorded with varying excitation wavelength are presented in Fig. 2C–F and S4. 2D RP perovskites with BA and BzA ligands show enhanced PL emission at 515–520 nm compared to DJ perovskites (Fig. 2C and E). However, 2D perovskite films with the BDA ligand were non-emissive (Fig. 2D). For all 2D films (except BDA), it was discernible that excitation of the exciton band at 440 nm yields the strongest PL emission, consistent with absorption spectra. It is interesting to note that the emission peak of 2D perovskites (with 50 : 50 Br : I) seen in Fig. 2 exhibits a large Stokes shift and resembles close to the emission peak seen with 2D iodide perovskite emission. As shown in Fig. S3, 2D bromide perovskite films exhibit pronounced PL emission around 400–410 nm and 2D iodide perovskite films at 510–525 nm. The alignment of the observed PL emission from all the 2D perovskites (with 50 : 50 Br : I) shows the formation of iodide-rich domains during the excitation of the film. As will be discussed in the following section, the mixed halide phase, upon photoirradiation, undergoes halide segregation, forming Br- and I-rich domains respectively. These segregated phases bring about red-shifted PL emission corresponding to the I-rich domain, as charge carrier funneling processes lead to their accumulation in the lower bandgap phase. In the case of PDMA, however, we observe PL emission from the mixed phase around 480 nm, thus indicating its resistance to photosegregation.

Photoinduced halide phase segregation in 2D perovskites

To further elucidate phase stability of the mixed halide 2D perovskites under photoirradiation, we tracked the absorption changes following the excitation with a continuous wave (CW) 405 nm diode laser (Fig. 3A). By tracking *in situ* spectral evolution under photoirradiation, it is possible to track the underlying impact of spacer cation molecules on the mixed halide phase stability. Bandgap excitation of 2D mixed halide perovskites facilitates the charge carrier generation, forming electron–hole pairs and accumulation of holes in iodide, initiating the halide ion migration and subsequent segregation (Fig. 3B). As a representative example of 2D perovskites, *in situ* absorption spectra changes were recorded using 2D mixed perovskite with a BA spacer cation over 15 min of irradiation (Fig. 3C). CW diode laser excitation induces the phase segregation to form Br- and I-rich domains (eqn (1)).[23]

$$2D\ BA_2PbBr_2I_2 + h\nu \rightarrow BA_2PbBr_4 + BA_2PbI_4\ (\text{fully segregated}) \quad (1)$$

As can be seen from the spectral changes, the mixed halide concentration as monitored from the absorbance at 450 nm decreases and new absorption features centered around 400 nm (Br-rich) and 500 nm (I-rich) concurrently emerges (Fig. 3C). Time-dependent spectral changes were captured through the

Open Access Article. Published on 21 1404. Downloaded on 28/11/1404 10:53:09 ..
This article is licensed under a Creative Commons Attribution-NonCommercial 3.0 Unported Licence.

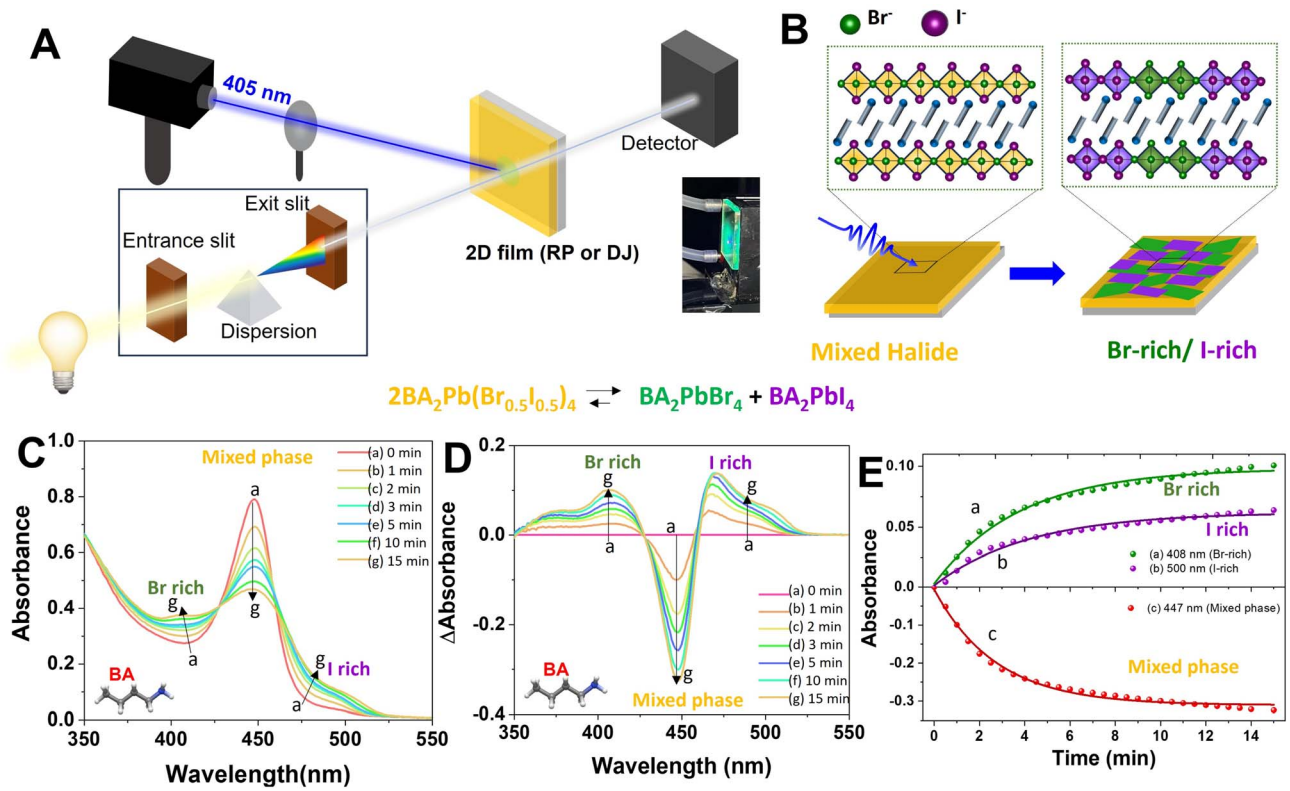

Fig. 3 (A) Schematic illustration of photoinduced halide segregation upon continuous wave light irradiation using a 405 nm diode laser (with a spot size of 0.764 cm^2) and corresponding *in situ* spectral absorption measurement. The inset in 3A shows a digital photo taken under photoirradiation using BA film. (B) Corresponding photoinduced halide ion segregation in the 2D mixed (Br : I = 50 : 50) halide perovskite films. (C and D) Time-dependent absorption changes (C) in 2D mixed halide perovskites with BA upon CW 405 nm diode laser irradiation (100 mW cm^{-2}) for 15 min and corresponding difference absorption (D) obtained by subtraction from the 0 min spectrum. (E) Kinetic trace and monoexponential fits by tracking the changes in Br-rich (at 408 m), mixed (at 447 nm), and I-rich (at 500 nm) domains, respectively, as shown in panel D. Note that the difference absorption spectra are obtained by subtracting the spectra recorded at longer time from the spectra at zero time.

difference absorption spectra (Fig. 3D). By tracking these absorption changes, one can analyze the kinetics of disappearance of parent mixed halide (447 nm) and formation of Br- (408 nm) and I-rich (500 nm) domains, respectively (Fig. 3E). The kinetic traces were fitted using a monoexponential function to obtain the kinetic rate constant (k). Since two molecules of 2D mixed halide perovskites undergo halide phase segregation, creating one molecule of each Br- and I-rich domain, the kinetic rate constant (k) of consumption of parent mixed halide was determined to be 6.1×10^{-3} s^{-1} (for mixed phase) that is almost double the k for the formation of the segregated phases (4.0×10^{-3} s^{-1} for Br- and I-rich domains), respectively, consistent with the eqn (1).[31] The photoluminescence (PL) emission measured during the photoirradiation shows a similar halide segregation trend (Fig. S5). Upon stopping the photoirradiation, the segregated 2D perovskite film recovers to restore the original mixed halide composition. Entropically driven halide mixing leads to its full recovery in the dark (Fig. S6A and B). It should be noted that it takes a longer time (around 180 minutes) to attain full recovery in the dark. The kinetic rate constant of dark recovery was determined to be 6.0×10^{-4} s^{-1}, which is an order of magnitude slower than the rate constant of photosegregation. (Fig. S6C).

The same photosegregation experiments were repeated using different spacer cation molecules such as BzA (RP), BDA (DJ), and PDMA (DJ), respectively, under the same laser power. Fig. 4A–F shows absorption (Fig. 4A–C) and corresponding difference absorption (Fig. 4D–F) spectral changes for 2D BzA (Fig. 4A and D), BDA (Fig. 4B and E), and PDMA (Fig. 4C and F), respectively. When subjected to CW laser irradiation (405 nm), other 2D perovskites are also susceptible to photoinduced halide segregation with the formation of Br- and I-rich phases, respectively. However, the magnitude and kinetics of photosegregation appear to be governed by the molecular structure and binding motif of the spacer cations. Interestingly, the magnitude of halide segregation, as can be seen in the difference absorption spectra, decreased from −0.35 (BA) to −0.05 (PDMA) (Fig. 4D–F). Compared to the linear BA-based 2D mixed halide perovskite, the aromatic BzA-based mixed halide perovskite film shows a decreased degree of segregation. The stronger binding energy of Pb–X within the same binding configuration of RP decreases the mobility of halides. Our previous studies also pointed out that the aromatic spacer cation such as phenethylamine (PEA) can prevent halide ion segregation compared to BA.[23] Recently, it was also shown that the melting point and disorder of the spacer cation molecule assembly in

© 2025 The Author(s). Published by the Royal Society of Chemistry

Open Access Article. Published on 21 1404. Downloaded on 28/11/1404 10:53:09 ..
This article is licensed under a Creative Commons Attribution-NonCommercial 3.0 Unported Licence.

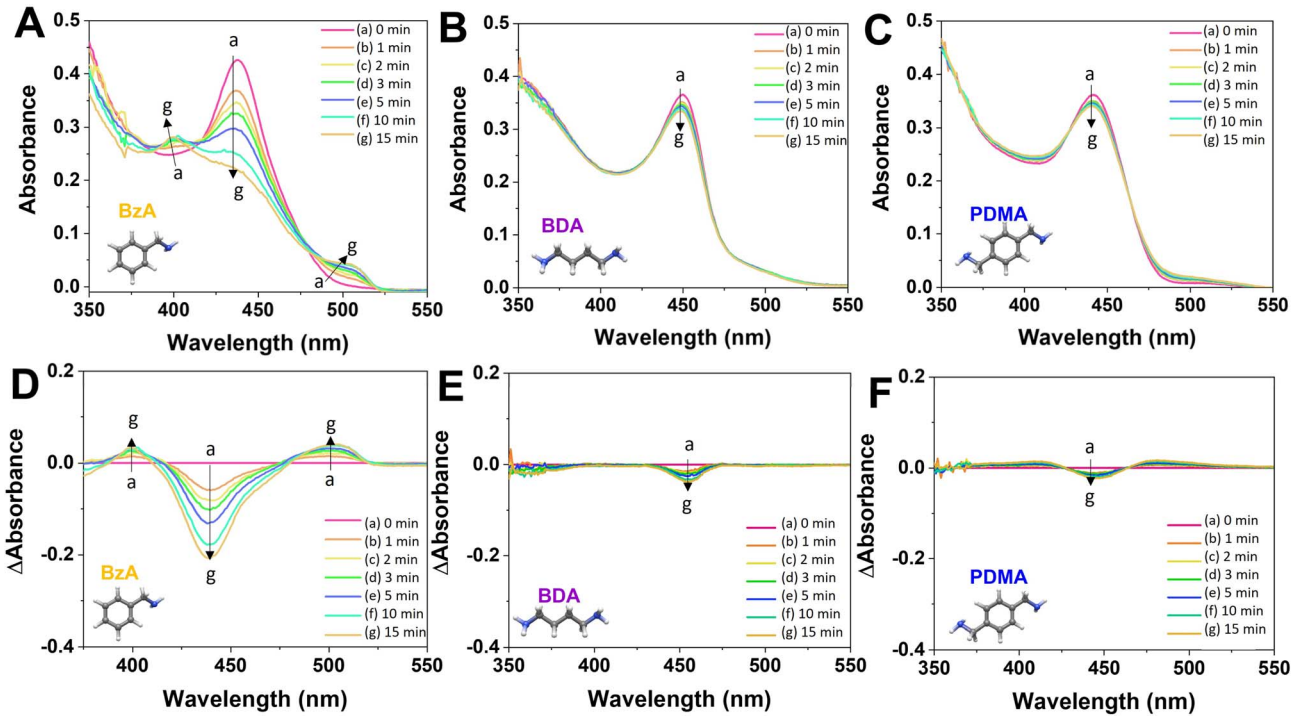

Fig. 4 (A–C) Time-dependent absorption changes and (D–F) corresponding difference absorption changes for 15 minutes recorded for 2D mixed halide perovskites with (A and D) BzA, (B and E) BDA, and (C and F) PDMA, respectively, upon CW 405 nm laser irradiation (100 mW cm^{-2}) for 15 minutes. In the difference absorption spectra, the 0 min spectrum serves as a reference spectrum for subtraction.

the 2D architectures indeed affect defect-mediated halide ion migration and mixing kinetics.[27] The enhanced intermolecular interactions in aromatic ligands due to π–π interactions, thus, play a crucial role in suppressing the halide ion migration by maintaining the 2D lattice frameworks.[70,71] When we further employ the DJ architecture with the BDA spacer, the halide segregations are mostly suppressed compared to 2D RP perovskites (Fig. 4B and E). The covalent tethering of DJ ligands atop the inorganic layer can indeed assemble more rigid 2D frameworks, which can more effectively suppress the halide phase segregation. The 2D perovskite with a PDMA spacer, which has both a DJ binding configuration and an aromatic ring, exhibits the most stable mixed halide phase upon photoirradiation among these four different spacer cations (Fig. 4C and F).

Role of spacer cations

We compared the kinetics of phase segregation in different 2D mixed halide perovskite films to evaluate the role of spacer cations on the photoinduced phase segregation (Fig. 5A and B). We further investigated the phenethylammonium (PEA) spacer cation, which is among the most commonly used in 2D perovskites (Fig. S7A and B).[23] There are two different aspects of these spacer cations that one needs to consider while evaluating the difference in the kinetics and degree of phase segregation. The first one is the aliphatic and aromatic nature of ligands. The rate constant of phase segregation decreased from 6.1×10^{-3} s^{-1} (for BA) to 1.9×10^{-3} s^{-1} (for PEA). The difference in the kinetic rate constant of phase segregation (k) among BA, BzA, and PEA with the same binding configuration as in 2D RP perovskite films arises mainly from the aromatic ring effect (Fig. 5B). Leung *et al.* also established the effect of alkyl chain length of aromatic spacer cations in stabilizing the mixed halide with photoirradiation, indicating that PEA is more stable than its BzA counterparts.[72,73] The longer alkyl chain in the PEA spacer cation provides greater conformational flexibility, thus improving van der Waals interactions of the spacer cation assembly. Increased spacer cation interactions reinforce the rigidity of 2D perovskite lattices, thereby more effectively suppressing halide segregation.[19,32,64] The second one is the nature of binding introduced through monovalent (RP type) and divalent (DJ type) spacer cations. The rate constant of phase segregation further decreased to 1.7×10^{-3} s^{-1} (for BDA) and to 9.3×10^{-4} s^{-1} (for PDMA), as illustrated in Fig. 5B and S7. An order of magnitude reduction observed in DJ perovskites relative to RP perovskites is mainly ascribed to the altered binding configuration of spacer cations.

We further repeated the photosegregation experiments using a lower light intensity of 40 mW cm^{-2} (Fig. S8). The degree of segregation ($\Delta A/A$ %) was obtained from the ratio of the decreased absorption of mixed halide perovskites and initial absorption intensity at 445 nm (Fig. S9). The degree of segregation decreased when the excitation intensity was lowered (Fig. 5C).

Quantum efficiency of halide segregation was further calculated using the equation Q. E. (%) = $(\eta_{mixed}/\eta_{photons}) \times 100$, where η_{mixed} is defined as the number of mixed halide molecules disappeared during photoirradiation and $\eta_{photons}$

Open Access Article. Published on 21 1404. Downloaded on 28/11/1404 10:53:09 ..
This article is licensed under a Creative Commons Attribution-NonCommercial 3.0 Unported Licence.

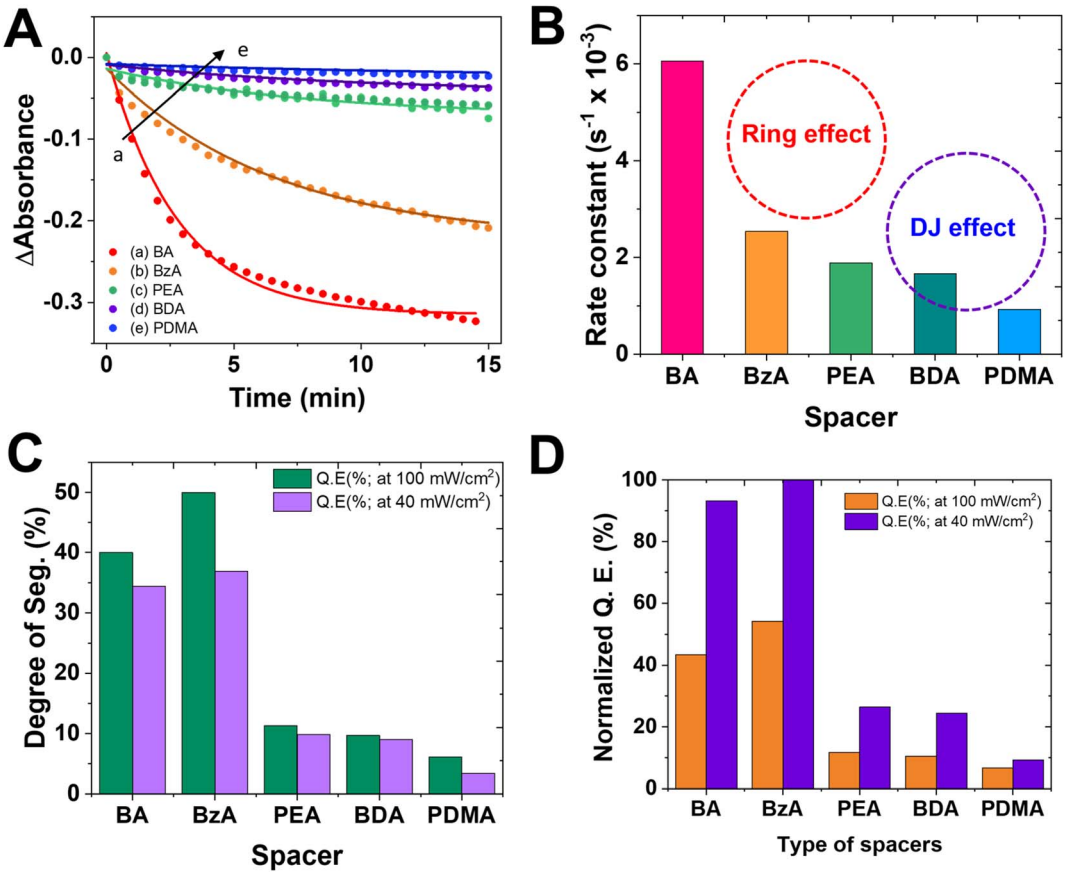

Fig. 5 (A) Tracking of difference absorption spectra at the mixed halide peak (at 445 nm) and kinetic fittings recorded for 2D mixed halide perovskite films with BA, BzA, BDA, PEA and PDMA. (B) Kinetic rate constant obtained from the monoexponential fits corresponding to the kinetics of disappearance of the mixed halide phase upon photoirradiation (100 mW cm^{-2}). (C) Degree of phase segregation plots for 2D perovskites with BA, BzA, BDA, PEA and PDMA, which is calculated by dividing the absorption intensity upon light irradiation by the initial absorption intensity at the mixed halide phase (440–450 nm). (D) Quantum efficiency calculation for 2D perovskites with BA, BzA, BDA, PEA and PDMA under light irradiation of 40 and 100 mW cm^{-2} for 15 min. In panel D, normalization was performed based on the highest Q. E. as 1.

corresponds to the number of molecules of incident photons (see the Experimental section for details). Upon photoirradiation with a CW 405 nm diode laser, the degree of phase segregation or disappearance of the mixed halide phase (η_{mixed}) relative to the number of photons explains how efficiently the mixed halide phase segregated into Br- and I-rich domains, respectively. The calculated efficiency at a given light intensity of 40 mW cm^{-2} indicates that Q. E. (%) significantly decreased from 4.2–4.5% (2D RP phases except PEA) to 0.4–1.1% (2D DJ phases) (Fig. S10). These observations demonstrate that the incident photons do not induce photosegregation in the DJ perovskites as effectively as in RP perovskites. In the case of PEA, the significantly reduced Q. E. (1.2%) is attributed to more rigidified 2D lattices. Since octahedral distortion plays a critical role in governing the defect-mediated halide ion migration, the rigidified 2D lattices formed through stronger van der Waals interactions arising from π–π aromatic stacking and the increased chain length of aromatic rings significantly suppress the extent of halide ion segregation under identical photoirradiation conditions. In addition, for all cases, segregation efficiency is less efficient in promoting the halide segregation at higher excitation intensity since the increased light intensity induced the increased charge carrier recombination, consistent with earlier reports (Fig. 5D).[30,32,74,75] It is worth noting that earlier studies have shown that such DJ perovskites with aromatic ring systems also underwent halide segregation when exposed to significantly extended photoirradiation.[72,76,77]

Excited state dynamics in 2D perovskites

The charge carrier generation in 2D halide perovskites is a primary event that influences the photoinduced halide segregation. Specifically, hole accumulation at I-rich sites leads to iodide oxidation and ion migration.[78–80] Using transient absorption spectroscopy (35 fs; 32 μJ cm^{-2}), we probed the excited state dynamics in the 2D mixed halide perovskites. Pulse laser excitation with 1 kHz frequency and a short pulse width of 35 fs does not induce phase segregation in mixed halide perovskite films. Thus, the mixed halide perovskites enable probing of the excited state behavior of 2D perovskite films using pump–probe measurements.

The time-resolved transient absorption spectra recorded at different delay times after 400 nm laser pulse excitation are

© 2025 The Author(s). Published by the Royal Society of Chemistry

Open Access Article. Published on 21 1404. Downloaded on 28/11/1404 10:53:09 ..
This article is licensed under a Creative Commons Attribution-NonCommercial 3.0 Unported Licence.

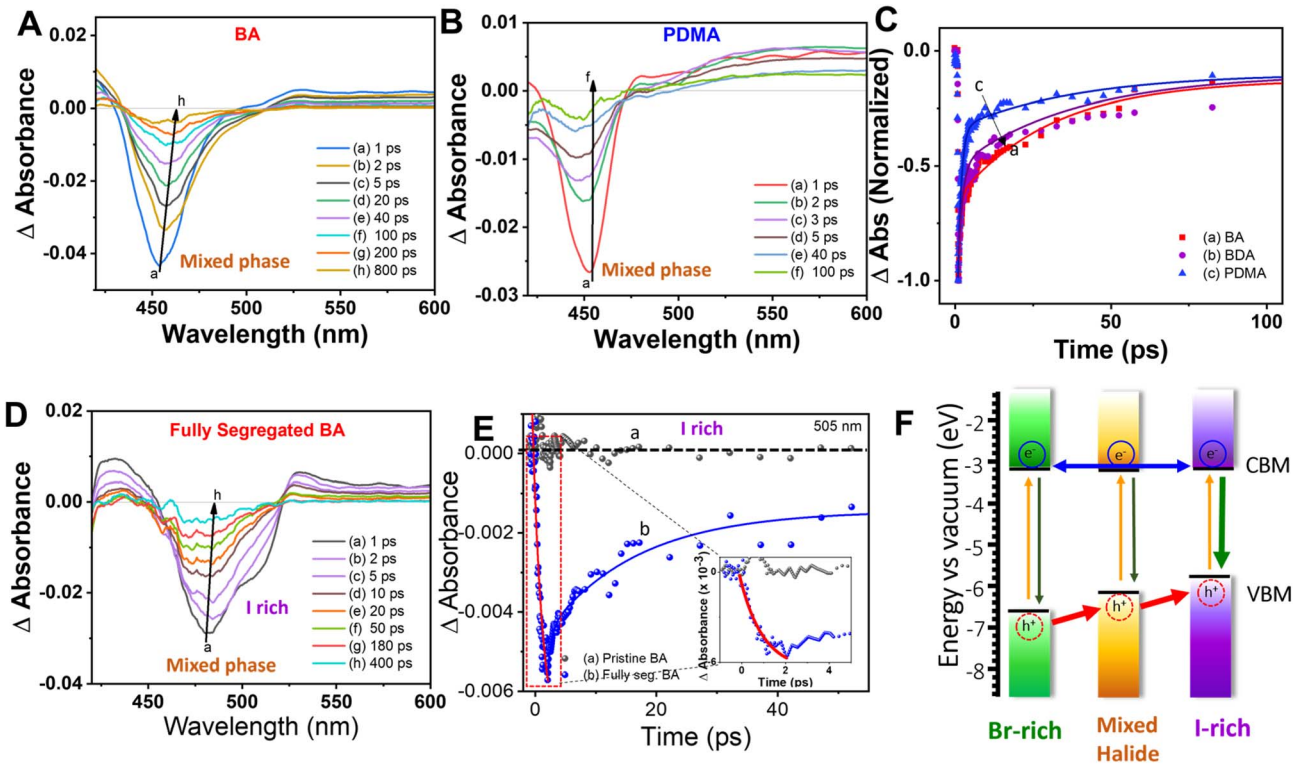

Fig. 6 (A and B) Time-resolved transient absorption spectra recorded following 400 nm laser pulse excitation (32 μJ cm^{-2}) of 2D mixed halide perovskite films with (A) BA and (B) PDMA. (C) Normalized bleach recovery profiles of 2D mixed halide perovskites with BA, BDA, and PDMA before 405 nm diode laser irradiation. (D) Time-resolved transient absorption spectra of 2D mixed halide perovskite films with BA after 405 nm laser diode excitation (25 mW cm^{-2}) for 10 min. (E) Bleach recovery profile at the I-rich domain peak (around 505 nm) recorded before (black) and after photoirradiation (blue) of 2D mixed halide perovskites with BA ligands. The inset of (E) shows the magnified kinetics at an earlier time scale of 0–5 ps. (F) Energy diagram of phase segregation and corresponding e–h transfer across the halide phases.

shown for 2D perovskite films with BA and PDMA spacer ligands (Fig. 6A and B). The transient absorption spectra were characterized by a pronounced bleach feature of the excitonic band at 445 nm along with a photoinduced absorption band at 500–700 nm. The former is ascribed to the ground state depopulation upon laser pulse excitation, and the latter is assigned to charge carrier filling in the excited state. The transient bleach recovery kinetics, analyzed using three different 2D-perovskite films with BA, BDA, and PDMA as spacer cations, are shown in Fig. 6C. The ground state bleach signal of 2D perovskites with BzA as spacer cations could not be recorded because of its instability during pump–probe laser measurements. The details of kinetic fitting parameters using a biexponential function are provided in Tables S2 and S3. The average excited state lifetimes as measured from the bleach recovery of perovskite films with different spacer cations were 58 ps (BA), 22 ps (BDA), and 8 ps (PDMA), respectively. The 2D DJ perovskites exhibit shorter excited state lifetimes as compared to 2D RP perovskites. Increased exciton binding energy in DJ perovskites, with a reduced van der Waals gap and increased dielectric confinement, is likely to lead to fast exciton/charge carrier recombination.[81]

We also examined the excited state behavior of the 2D perovskite films following photoirradiation for 10 min. For DJ mixed halide perovskite (BDA and PDMA as spacer cations) films, which were preirradiated with a CW 405 nm laser for 10 min, the transient absorption spectra show minimal changes resulting from photoirradiation (Fig. S11). These results mirror the suppressed halide segregation seen with steady-state absorption measurements. The bleach recovery kinetics of these films (before and after photoirradiation) are similar, indicating that the 2D films with these spacer cations do not undergo noticeable phase segregation. In contrast, pre-irradiated 2D perovskites with BA spacer cations exhibit additional bleach around 510 nm (Fig. 6D). The two bleach features of the transient spectra, centered at around 445 nm (mixed halide) and 510 nm, correspond to residual mixed halide and I-rich domains in the photoirradiated film (the excitation of 400 nm in the set-up does not allow detecting the Br-rich domain (408 nm) due to spectral overlap with the pump). The bleach recovery recorded at 510 nm, corresponding to the iodide-rich domain, exhibits an average lifetime of 12 ps. It is also interesting to note a growth in the bleach (lifetime ~2 ps), which we attribute to the charge carrier flow from Br-rich and mixed halide domains to I-rich regions (Fig. 6E and F). More details on the charge carrier funneling from larger bandgap perovskite regions to low bandgap iodide regions can be found elsewhere.[28,29,80,82–84]

The excitonic binding energy of 2D perovskites is proportional to the dielectric constant of the 2D inorganic halide slab, thus increasing from $(PEA)_2PbBr_4$ (335 meV) to $(PEA)_2PbI_4$ (453

Open Access Article. Published on 21 1404. Downloaded on 28/11/1404 10:53:09 ..
This article is licensed under a Creative Commons Attribution-NonCommercial 3.0 Unported Licence.

meV).[81] Greater dielectric contrast between the organic and inorganic layers in 2D iodide perovskites increases the dielectric confinement effect, thus accelerating electron–hole recombination. As seen from the 2D PL excitation–emission spectra, the 2D iodide serves as the main charge carrier recombination channel owing to thermodynamically favorable charge transfer (Fig. S3 and S4). When tracking the ground state bleach recovery of the mixed halide perovskites before and after photoirradiation, the segregated film shows faster bleach recovery with an average lifetime of 25 ps due to cascade charge transfer (Fig. S12).

In summary, the molecular structure and binding configuration of spacer cation molecules incorporated into the 2D halide perovskite frameworks influence the phase segregation of mixed halide under photoirradiation. The photosegregation can be analyzed by tracking the spectral absorption changes of 2D mixed halide perovskites with different spacer cations (BA, BzA, BDA, and PDMA), ranging from linear (BA and BDA) to aromatic (BzA and PDMA) molecules across both RP and DJ perovskites. The incorporation of aromatic rings and switching to more covalent DJ frameworks indeed is effective in suppressing the photoinduced halide segregation. The results presented in this study provide new insights into the design principles of the spacer cation molecules for constructing stable quasi-2D or 2D/3D perovskite solar cells.

Author contributions

All authors were involved in the conceptualization and execution of the research, in the interpretation of the findings, and in the preparation of the manuscript. S. Min, M. Mukherjee, and G. Szabó carried out experiments and corresponding data analysis. J. Cho and P. V. Kamat conceived the idea and supervised the overall project.

Conflicts of interest

The authors declare no conflict of interest.

Data availability

The data supporting this article have been included as part of the supplementary information (SI). Supplementary information: XPS spectra, SEM images, UV-vis absorption spectra, PL emission spectra, 2D excitation–emission spectra, quantum efficiency calculation, and transient absorption spectra. See DOI: **https://doi.org/10.1039/d5sc06511a**.

Acknowledgements

J. Cho acknowledges the support from the National Research Foundation of Korea (NRF) grant funded by the Korea government (MSIT) (NRF-2022R1C1C1004131) to conduct the research. P. V. Kamat acknowledges the support from the Division of Materials Sciences and Engineering Office of Basic Energy Sciences of the U.S. Department of Energy through Award DE-SC0014334. This is contribution number No. 5481 from the Notre Dame Radiation Laboratory.

References

1 G. Grancini and M. K. Nazeeruddin, Dimensional Tailoring of Hybrid Perovskites for Photovoltaics, *Nat. Rev. Mater.*, 2019, **4**(1), 4–22.
2 X. Zhao, T. Liu and Y. L. Loo, Advancing 2D Perovskites for Efficient and Stable Solar Cells: Challenges and Opportunities, *Adv. Mater.*, 2022, **34**(3), 1–19.
3 S. D. Baek, S. J. Yang, H. Yang, W. Shao, Y. T. Yang and L. Dou, Exciton Dynamics in Layered Halide Perovskite Light-Emitting Diodes, *Adv. Mater.*, 2024, 1–24.
4 S. J. Yang, K. Wang, Y. Luo, J. Y. Park, H. Yang, A. H. Coffey, K. Ma, J. Sun, S. Wieghold, C. Zhu and L. Dou, Two-Factor Phase Separations in Mixed-Halide Quasi-2D Perovskite LEDs: Dimensionality and Halide Segregations, *ACS Energy Lett.*, 2023, **8**(9), 3693–3701.
5 Y. Li, Y. Lei, H. Wang and Z. Jin, Two-Dimensional Metal Halides for X-Ray Detection Applications, *Nano-Micro Lett.*, 2023, **15**(1), 1–18.
6 K. Leng, W. Fu, Y. Liu, M. Chhowalla and K. P. Loh, From Bulk to Molecularly Thin Hybrid Perovskites, *Nat. Rev. Mater.*, 2020, **5**(7), 482–500.
7 P. Wangyang, C. Gong, G. Rao, K. Hu, X. Wang, C. Yan, L. Dai, C. Wu and J. Xiong, Recent Advances in Halide Perovskite Photodetectors Based on Different Dimensional Materials, *Adv. Opt. Mater.*, 2018, **6**(11), 1–30.
8 D. Powell, K. R. Hansen, L. Flannery and L. Whittaker-Brooks, Traversing Excitonic and Ionic Landscapes: Reduced-Dimensionality-Inspired Design of Organometal Halide Semiconductors for Energy Applications, *Acc. Chem. Res.*, 2021, **54**(23), 4371–4382.
9 J. V. Milić, S. M. Zakeeruddin and M. Grätzel, Layered Hybrid Formamidinium Lead Iodide Perovskites: Challenges and Opportunities, *Acc. Chem. Res.*, 2021, **54**(12), 2729–2740.
10 J. V. Passarelli, C. M. Mauck, S. W. Winslow, C. F. Perkinson, J. C. Bard, H. Sai, K. W. Williams, A. Narayanan, D. J. Fairfield, M. P. Hendricks, W. A. Tisdale and S. I. Stupp, Tunable Exciton Binding Energy in 2D Hybrid Layered Perovskites through Donor–Acceptor Interactions within the Organic Layer, *Nat. Chem.*, 2020, **12**(8), 672–682.
11 G. Szabó and P. V. Kamat, How Cation Migration across a 2D/3D Interface Dictates Perovskite Solar Cell Efficiency, *ACS Energy Lett.*, 2024, **9**(1), 193–200.
12 H. Tsai, W. Nie, J. C. Blancon, C. C. Stoumpos, C. M. M. Soe, J. Yoo, J. Crochet, S. Tretiak, J. Even, A. Sadhanala, G. Azzellino, R. Brenes, P. M. Ajayan, V. Bulović, S. D. Stranks, R. H. Friend, M. G. Kanatzidis and A. D. Mohite, Stable Light-Emitting Diodes Using Phase-Pure Ruddlesden–Popper Layered Perovskites, *Adv. Mater.*, 2018, **30**(6), 1–9.
13 H. Tsai, W. Nie, J. C. Blancon, C. C. Stoumpos, R. Asadpour, B. Harutyunyan, A. J. Neukirch, R. Verduzco, J. J. Crochet, S. Tretiak, L. Pedesseau, J. Even, M. A. Alam, G. Gupta, J. Lou, P. M. Ajayan, M. J. Bedzyk, M. G. Kanatzidis and

© 2025 The Author(s). Published by the Royal Society of Chemistry

Open Access Article. Published on 21 1404. Downloaded on 28/11/1404 10:53:09 ..
This article is licensed under a Creative Commons Attribution-NonCommercial 3.0 Unported Licence.

A. D. Mohite, High-Efficiency Two-Dimensional Ruddlesden-Popper Perovskite Solar Cells, *Nature*, 2016, **536**(7616), 312–317.

14 E. S. Vasileiadou, B. Wang, I. Spanopoulos, I. Hadar, A. Navrotsky and M. G. Kanatzidis, Insight on the Stability of Thick Layers in 2D Ruddlesden-Popper and Dion-Jacobson Lead Iodide Perovskites, *J. Am. Chem. Soc.*, 2021, **143**(6), 2523–2536.

15 L. Mao, C. C. Stoumpos and M. G. Kanatzidis, Two-Dimensional Hybrid Halide Perovskites: Principles and Promises, *J. Am. Chem. Soc.*, 2019, **141**(3), 1171–1190.

16 J. Cho, P. S. Mathew, J. T. DuBose and P. V. Kamat, Photoinduced Halide Segregation in Ruddlesden–Popper 2D Mixed Halide Perovskite Films, *Adv. Mater.*, 2021, **33**(48), 1–8.

17 N. Mercier, Hybrid Halide Perovskites: Discussions on Terminology and Materials, *Angew. Chem., Int. Ed.*, 2019, **58**(50), 17912–17917.

18 X. Li, J. M. Hoffman and M. G. Kanatzidis, The 2D Halide Perovskite Rulebook: How the Spacer Influences Everything from the Structure to Optoelectronic Device Efficiency, *Chem. Rev.*, 2021, **121**(4), 2230–2291.

19 X. Gao, Y. Wu, Y. Zhang, X. Chen, Z. Song, T. Zhang, Q. Fang, Q. Ji, M. G. Ju and J. Wang, How the Spacer Influences the Stability of 2D Perovskites?, *Small Methods*, 2025, **9**(5), 1–9.

20 J. Cho, J. T. Dubose and P. V. Kamat, Charge Carrier Recombination Dynamics of Two-Dimensional Lead Halide Perovskites, *J. Phys. Chem. Lett.*, 2020, **11**(7), 2570–2576.

21 K. R. Hansen, C. Y. Wong, C. E. McClure, B. Romrell, L. Flannery, D. Powell, K. Garden, A. Berzansky, M. Eggleston, D. J. King, C. M. Shirley, M. C. Beard, W. Nie, A. Schleife, J. S. Colton and L. Whittaker-Brooks, Mechanistic Origins of Excitonic Properties in 2D Perovskites: Implications for Exciton Engineering, *Matter*, 2023, **6**(10), 3463–3482.

22 C. M. Mauck and W. A. Tisdale, Excitons in 2D Organic–Inorganic Halide Perovskites, *Trends Chem.*, 2019, **1**(4), 380–393.

23 P. S. Mathew, J. T. Dubose, J. Cho, P. V. Kamat, J. T. Dubose, J. Cho and P. V. Kamat, Spacer Cations Dictate Photoinduced Phase Segregation in 2D Mixed Halide Perovskites, *ACS Energy Lett.*, 2021, **6**(7), 2499–2501.

24 P. S. Mathew, G. Szabó, M. Kuno and P. V. Kamat, Phase Segregation and Sequential Expulsion of Iodide and Bromide in Photoirradiated Ruddlesden-Popper 2D Perovskite Films, *ACS Energy Lett.*, 2022, **7**(11), 3982–3988.

25 A. N. Yadav, S. Min, H. Choe, J. Park and J. Cho, Halide Ion Mixing across Colloidal 2D Ruddlesden-Popper Perovskites: Implication of Spacer Ligand on Mixing Kinetics, *Small*, 2023, **20**, 2305546.

26 S. Min and J. Cho, Halide Ion Mobility in Paired 2D Halide Perovskites: Ruddlesden–Popper Versus Dion–Jacobson Phases, *Adv. Opt. Mater.*, 2024, **12**(12), 1–10.

27 S. Min, S. Park, Y. H. Lee, D. Kim and J. Cho, Halide Ion Exchange Mechanisms in 2D Ruddlesden-Popper Perovskites : Diffusion- vs Reaction-Limited, *Small*, 2025, 1–11.

28 S. J. Yoon, S. Draguta, J. S. Manser, O. Sharia, W. F. Schneider, M. Kuno and P. V. Kamat, Tracking Iodide and Bromide Ion Segregation in Mixed Halide Lead Perovskites during Photoirradiation, *ACS Energy Lett.*, 2016, **1**(1), 290–296.

29 S. J. Yoon, M. Kuno and P. V. Kamat, Shift Happens. How Halide Ion Defects Influence Photoinduced Segregation in Mixed Halide Perovskites, *ACS Energy Lett.*, 2017, **2**(7), 1507–1514.

30 T. Elmelund, B. Seger, M. Kuno and P. V. Kamat, How Interplay between Photo and Thermal Activation Dictates Halide Ion Segregation in Mixed Halide Perovskites, *ACS Energy Lett.*, 2020, **5**(1), 56–63.

31 J. Cho and P. V. Kamat, How Chloride Suppresses Photoinduced Phase Segregation in Mixed Halide Perovskites, *Chem. Mater.*, 2020, **32**(14), 6206–6212.

32 J. Cho and P. V. Kamat, Photoinduced Phase Segregation in Mixed Halide Perovskites: Thermodynamic and Kinetic Aspects of Cl–Br Segregation, *Adv. Opt. Mater.*, 2020, 1–9.

33 Y. Hassan, J. H. Park, M. L. Crawford, A. Sadhanala, J. Lee, J. C. Sadighian, E. Mosconi, R. Shivanna, E. Radicchi, M. Jeong, C. Yang, H. Choi, S. H. Park, M. H. Song, F. De Angelis, C. Y. Wong, R. H. Friend, B. R. Lee and H. J. Snaith, Ligand-Engineered Bandgap Stability in Mixed-Halide Perovskite LEDs, *Nature*, 2021, **591**(7848), 72–77.

34 Z. Huang, A. H. Proppe, H. Tan, M. I. Saidaminov, F. Tan, A. Mei, C. S. Tan, M. Wei, Y. Hou, H. Han, S. O. Kelley and E. H. Sargent, Suppressed Ion Migration in Reduced-Dimensional Perovskites Improves Operating Stability, *ACS Energy Lett.*, 2019, **4**(7), 1521–1527.

35 G. F. Samu, C. Janáky and P. V. Kamat, A Victim of Halide Ion Segregation. How Light Soaking Affects Solar Cell Performance of Mixed Halide Lead Perovskites, *ACS Energy Lett.*, 2017, **2**(8), 1860–1861.

36 L. Hu, X. Guan, W. Chen, Y. Yao, T. Wan, C. H. Lin, N. D. Pham, L. Yuan, X. Geng, F. Wang, C. Y. Huang, J. Yuan, S. Cheong, R. D. Tilley, X. Wen, D. Chu, S. Huang and T. Wu, Linking Phase Segregation and Photovoltaic Performance of Mixed-Halide Perovskite Films through Grain Size Engineering, *ACS Energy Lett.*, 2021, **6**(4), 1649–1658.

37 J. Cho, J. T. Dubose, A. N. T. Le and P. V. Kamat, Suppressed Halide Ion Migration in 2D Lead Halide Perovskites, *ACS Mater. Lett.*, 2020, **2**(6), 565–570.

38 L. N. Quan, M. Yuan, R. Comin, O. Voznyy, E. M. Beauregard, S. Hoogland, A. Buin, A. R. Kirmani, K. Zhao, A. Amassian, D. H. Kim and E. H. Sargent, Ligand-Stabilized Reduced-Dimensionality Perovskites, *J. Am. Chem. Soc.*, 2016, **138**(8), 2649–2655.

39 Q. Zhang, E. Linardy, X. Wang and G. Eda, Excitonic Energy Transfer in Heterostructures of Quasi-2D Perovskite and Monolayer WS2, *ACS Nano*, 2020, **14**(9), 11482–11489.

40 H. Choe, D. Jeon, S. J. Lee and J. Cho, Mixed or Segregated: Toward Efficient and Stable Mixed Halide Perovskite-Based Devices, *ACS Omega*, 2021, **6**(38), 24304–24315.

Open Access Article. Published on 21 1404. Downloaded on 28/11/1404 10:53:09 ..
This article is licensed under a Creative Commons Attribution-NonCommercial 3.0 Unported Licence.

41 P. S. Mathew, P. S. Mathew, G. F. Samu, G. F. Samu, C. Janáky, P. V. Kamat, P. V. Kamat and P. V. Kamat, Iodine (I) Expulsion at Photoirradiated Mixed Halide Perovskite Interface. Should i Stay or Should i Go?, *ACS Energy Lett.*, 2020, **5**(6), 1872–1880.
42 P. Susan, P. Mathew, J. Cho and P. V. Kamat, Ramifications of Ion Migration in 2D Lead Halide Perovskites, *ACS Energy Lett.*, 2024, **9**(3), 1103–1114.
43 J. T. Dubose, P. S. Mathew, J. Cho, M. Kuno and P. V. Kamat, Modulation of Photoinduced Iodine Expulsion in Mixed Halide Perovskites with Electrochemical Bias, *J. Phys. Chem. Lett.*, 2021, **12**(10), 2615–2621.
44 A. J. Knight, J. Borchert, R. D. J. Oliver, J. B. Patel, P. G. Radaelli, H. J. Snaith, M. B. Johnston and L. M. Herz, Halide Segregation in Mixed-Halide Perovskites: Influence of A-Site Cations, *ACS Energy Lett.*, 2021, **6**(2), 799–808.
45 K. O. Ighodalo, W. Chen, Z. Liang, Y. Shi, S. Chu, Y. Zhang, R. Khan, H. Zhou, X. Pan, J. Ye and Z. Xiao, Negligible Ion Migration in Tin-Based and Tin-Doped Perovskites, *Angew. Chem., Int. Ed.*, 2023, **62**(5), e202213932.
46 Z. Le, A. Liu, Y. Reo, S. Bai, Y. Y. Noh and H. Zhu, Ion Migration in Tin-Halide Perovskites, *ACS Energy Lett.*, 2024, 1639–1644.
47 J. Cho, J. T. Dubose, P. S. Mathew and P. V. Kamat, Electrochemically Induced Iodine Migration in Mixed Halide Perovskites: Suppression through Chloride Insertion, *Chem. Commun.*, 2021, **57**(2), 235–238.
48 R. A. Belisle, K. A. Bush, L. Bertoluzzi, A. Gold-Parker, M. F. Toney and M. D. McGehee, Impact of Surfaces on Photoinduced Halide Segregation in Mixed-Halide Perovskites, *ACS Energy Lett.*, 2018, **3**(11), 2694–2700.
49 S. Martani, Y. Zhou, I. Poli, E. Aktas, D. Meggiolaro, J. Jiménez-López, E. L. Wong, L. Gregori, M. Prato, D. Di Girolamo, A. Abate, F. De Angelis and A. Petrozza, Defect Engineering to Achieve Photostable Wide Bandgap Metal Halide Perovskites, *ACS Energy Lett.*, 2023, **8**(6), 2801–2808.
50 X. Shen, K. Kang, Z. Yu, W. H. Jeong, H. Choi, S. H. Park, S. D. Stranks, H. J. Snaith, R. H. Friend and B. R. Lee, Passivation Strategies for Mitigating Defect Challenges in Halide Perovskite Light-Emitting Diodes, *Joule*, 2023, **7**(2), 272–308.
51 N. T. P. Hartono, J. Thapa, A. Tiihonen, F. Oviedo, C. Batali, J. J. Yoo, Z. Liu, R. Li, D. F. Marrón, M. G. Bawendi, T. Buonassisi and S. Sun, How Machine Learning Can Help Select Capping Layers to Suppress Perovskite Degradation, *Nat. Commun.*, 2020, **11**(1), 1–9.
52 G. F. Samu, Á. Balog, F. De Angelis, D. Meggiolaro, P. V. Kamat and C. Janáky, Electrochemical Hole Injection Selectively Expels Iodide from Mixed Halide Perovskite Films, *J. Am. Chem. Soc.*, 2019, **141**(27), 10812–10820.
53 J. Cho, J. T. Dubose and P. V. Kamat, Charge Injection from Excited Cs2AgBiBr6 Quantum Dots into Semiconductor Oxides, *Chem. Mater.*, 2020, **32**(1), 510–517.
54 G. Y. Kim, A. Senocrate, T. Y. Yang, G. Gregori, M. Grätzel and J. Maier, Large Tunable Photoeffect on Ion Conduction in Halide Perovskites and Implications for Photodecomposition, *Nat. Mater.*, 2018, **17**(5), 445–449.
55 Z. Xu, R. A. Kerner, L. Kronik and B. P. Rand, Beyond Ion Migration in Metal Halide Perovskites: Toward a Broader Photoelectrochemistry Perspective, *ACS Energy Lett.*, 2024, 4645–4654.
56 Z. Xu, R. A. Kerner, J. J. Berry and B. P. Rand, Iodine Electrochemistry Dictates Voltage-Induced Halide Segregation Thresholds in Mixed-Halide Perovskite Devices, *Adv. Funct. Mater.*, 2022, **32**(33), 2203432.
57 R. A. Kerner, Z. Xu, B. W. Larson and B. P. Rand, The Role of Halide Oxidation in Perovskite Halide Phase Separation, *Joule*, 2021, **5**(9), 2273–2295.
58 R. F. Moral, C. A. R. Perini, T. Kodalle, A. Kim, F. Babbe, N. Harada, J. Hajhemati, P. Schulz, N. S. Ginsberg, S. Aloni, C. P. Schwartz, J. P. Correa-Baena and C. M. Sutter-Fella, Anion and Cation Migration at 2D/3D Halide Perovskite Interfaces, *ACS Energy Lett.*, 2024, **9**(6), 2703–2716.
59 C. Liu, Y. Yang, J. D. Fletcher, A. Liu, I. W. Gilley, C. B. Musgrave, Z. Wang, H. Zhu, H. Chen, R. P. Reynolds, B. Ding, Y. Ding, X. Zhang, R. Skackauskaite, H. Wan, L. Zeng, A. S. R. Bati, N. Shibayama, V. Getautis, B. Chen, K. Rakstys, P. J. Dyson, M. G. Kanatzidis, E. H. Sargent and M. K. Nazeeruddin, Cation Interdiffusion Control for 2D/3D Heterostructure Formation and Stabilization in Inorganic Perovskite Solar Modules, *Nat. Energy*, 2025, **10**, 981–990.
60 M. P. Arciniegas and L. Manna, Designing Ruddlesden-Popper Layered Perovskites through Their Organic Cations, *ACS Energy Lett.*, 2022, 2944–2953.
61 A. Singh and D. B. Mitzi, Emergence of Melt and Glass States of Halide Perovskite Semiconductors, *Nat. Rev. Mater.*, 2025, **10**(3), 211–227.
62 A. Singh, Y. Xie, C. Adams, B. G. Bobay and D. B. Mitzi, Controlling Glass Forming Kinetics in 2D Perovskites Using Organic Cation Isomers, *Chem. Sci.*, 2024, **15**(17), 6432–6444.
63 R. L. Kingsford, S. R. Jackson, L. C. Bloxham and C. G. Bischak, Controlling Phase Transitions in Two-Dimensional Perovskites through Organic Cation Alloying, *J. Am. Chem. Soc.*, 2023, **145**(21), 11773–11780.
64 P. K. Rajput, P. Salunkhe, M. Sarma, M. Basu, A. Gopal, A. Joshi, A. S. Shingote, S. Saha, A. Rahman and A. Nag, Entropy-Driven Reversible Melting and Recrystallization of Layered Hybrid Perovskites, *Small*, 2024, 1–9.
65 N. S. Dahod, W. Paritmongkol, A. Stollmann, C. Settens, S. L. Zheng and W. A. Tisdale, Melting Transitions of the Organic Subphase in Layered Two-Dimensional Halide Perovskites, *J. Phys. Chem. Lett.*, 2019, **10**(11), 2924–2930.
66 K. R. Hansen, C. E. McClure, M. A. Parker, Z. Xie, W. Nie, J. S. Colton and L. Whittaker-Brooks, Stochastic Charge-Transfer Excitons in 2D Metal-Halide Perovskites, *ACS Energy Lett.*, 2024, **9**(4), 1645–1653.
67 S. G. Motti, M. Kober-Czerny, M. Righetto, P. Holzhey, J. Smith, H. Kraus, H. J. Snaith, M. B. Johnston and L. M. Herz, Exciton Formation Dynamics and Band-Like Free Charge-Carrier Transport in 2D Metal Halide

© 2025 The Author(s). Published by the Royal Society of Chemistry

Open Access Article. Published on 21 1404. Downloaded on 28/11/1404 10:53:09 ..
This article is licensed under a Creative Commons Attribution-NonCommercial 3.0 Unported Licence.

Perovskite Semiconductors, *Adv. Funct. Mater.*, 2023, **33**(32), 2300363.

68 E. Shi and L. Dou, Halide Perovskite Epitaxial Heterostructures, *Accounts Mater. Res.*, 2020, **1**(3), 213–224.

69 X. Xiao, J. Dai, Y. Fang, J. Zhao, X. Zheng, S. Tang, P. N. Rudd, X. C. Zeng and J. Huang, Suppressed Ion Migration along the In-Plane Direction in Layered Perovskites, *ACS Energy Lett.*, 2018, **3**(3), 684–688.

70 E. Shi, B. Yuan, S. B. Shiring, Y. Gao, Akriti, Y. Guo, C. Su, M. Lai, P. Yang, J. Kong, B. M. Savoie, Y. Yu and L. Dou, Two-Dimensional Halide Perovskite Lateral Epitaxial Heterostructures, *Nature*, 2020, **580**(7805), 614–620.

71 E. Mosconi, A. A. Alothman, R. Long, W. Kaiser and F. De Angelis, Intermolecular Interactions of A-Site Cations Modulate Stability of 2D Metal Halide Perovskites, *ACS Energy Lett.*, 2023, **8**(1), 748–752.

72 A. Dučinskas, G. C. Fish, M. A. Hope, L. Merten, D. Moia, A. Hinderhofer, L. C. Carbone, J. E. Moser, F. Schreiber, J. Maier, J. V. Milić and M. Grätzel, The Role of Alkyl Chain Length and Halide Counter Ion in Layered Dion-Jacobson Perovskites with Aromatic Spacers, *J. Phys. Chem. Lett.*, 2021, **12**(42), 10325–10332.

73 T. L. Leung, Z. Ren, A. A. Syed, L. Grisanti, A. B. Djurišić and J. Popović, Photoinduced Segregation Behavior in 2D Mixed Halide Perovskite: Effects of Light and Heat, *ACS Energy Lett.*, 2022, **7**(10), 3500–3508.

74 S. Draguta, O. Sharia, S. J. Yoon, M. C. Brennan, Y. V. Morozov, J. M. Manser, P. V. Kamat, W. F. Schneider and M. Kuno, Rationalizing the Light-Induced Phase Separation of Mixed Halide Organic-Inorganic Perovskites, *Nat. Commun.*, 2017, **8**(1), 200.

75 M. C. Brennan, A. Ruth, P. V. Kamat and M. Kuno, Photoinduced Anion Segregation in Mixed Halide Perovskites, *Trends Chem.*, 2020, **2**(4), 282–301.

76 Y. R. Wang, A. Senocrate, M. Mladenović, A. Dučinskas, G. Y. Kim, U. Rothlisberger, J. V. Milić, D. Moia, M. Grätzel and J. Maier, Photo De-Mixing in Dion-Jacobson 2D Mixed Halide Perovskites, *Adv. Energy Mater.*, 2022, **12**(26), 2200768.

77 A. Dučinskas, M. Jung, Y. R. Wang, J. V. Milić, D. Moia, M. Grätzel and J. Maier, Mixed Ionic-Electronic Conduction in Ruddlesden-Popper and Dion-Jacobson Layered Hybrid Perovskites with Aromatic Organic Spacers, *J. Mater. Chem. C*, 2024, **12**(22), 7909–7915.

78 Z. Xu, R. A. Kerner, S. P. Harvey, K. Zhu, J. J. Berry and B. P. Rand, Halogen Redox Shuttle Explains Voltage-Induced Halide Redistribution in Mixed-Halide Perovskite Devices, *ACS Energy Lett.*, 2023, **8**(1), 513–520.

79 S. Min, M. Jeon, J. Cho, J. H. Bang and P. V. Kamat, Spectroelectrochemical Insights into the Intrinsic Nature of Lead Halide Perovskites, *Nano Converg.*, 2024, **11**(1), 49.

80 J. T. Dubose and P. V. Kamat, Hole Trapping in Halide Perovskites Induces Phase Segregation, *Accounts Mater. Res.*, 2022, **3**(7), 761–771.

81 R. Chakraborty and A. Nag, Correlation of Dielectric Confinement and Excitonic Binding Energy in 2D Layered Hybrid Perovskites Using Temperature Dependent Photoluminescence, *J. Phys. Chem. C*, 2020, **124**(29), 16177–16185.

82 P. V. Kamat and M. Kuno, Halide Ion Migration in Perovskite Nanocrystals and Nanostructures, *Acc. Chem. Res.*, 2021, **54**(3), 520–531.

83 J. S. Manser, J. A. Christians and P. V. Kamat, Intriguing Optoelectronic Properties of Metal Halide Perovskites, *Chem. Rev.*, 2016, **116**(21), 12956–13008.

84 J. M. Frost and A. Walsh, What Is Moving in Hybrid Halide Perovskite Solar Cells?, *Acc. Chem. Res.*, 2016, **49**(3), 528–535.